Highly Selective Homogeneous Ethylene Epoxidation in Gas (Ethylene)-Expanded Liquid: Transport and Kinetic Studies

Madhav Ghanta and Bala Subramaniam
Dept. of Chemical and Petroleum Engineering, Center for Environmentally Beneficial Catalysis, University of Kansas, Lawrence, KS 66045

Hyun-Jin Lee and Daryle H. Busch
Dept. of Chemistry, Center for Environmentally Beneficial Catalysis, University of Kansas, Lawrence, KS 66045

DOI 10.1002/aic.13789
Published online April 17, 2012 in Wiley Online Library (wileyonlinelibrary.com).

Recently a homogeneous liquid-phase ethylene oxide (EO) process with nearly total EO selectivity, catalyzed by methyltrioxorhenium with H_2O_2 as an oxidant, was reported. Fundamental mass transfer and kinetic studies of this reaction are reported in the present work. Volumetric expansion studies revealed that the liquid reaction phase (methanol + H_2O_2/H_2O) is expanded by up to 12% by compressed ethylene in the 20–40°C range and up to 50 bars. This represents an increase in ethylene solubility by approximately one-order of magnitude, attributed to the unique exploitation of near-critical ethylene ($P_c = 50.76$ bar; $T_c = 9.5$°C). Interphase mass-transfer coefficients for ethylene dissolution into the liquid phase were obtained experimentally. Operating at conditions that enhanced the ethylene solubility and *eliminated interphase mass-transfer limitations maximized the EO productivity (1.61–4.97 g EO/h/g cat), rendering it comparable to the conventional process. Intrinsic kinetic parameters, estimated from fixed-time semibatch reactor studies, disclosed the moderate activation energy (57 ± 2 kJ/mol).* © 2012 American Institute of Chemical Engineers *AIChE J,* 59: 180–187, 2013

Keywords: epoxidation, methyltrioxorhenium, hydrogen peroxide, gas-expanded liquid

Introduction

Ethylene oxide (EO), a bulk intermediate chemical, has a worldwide demand that is growing at 6–7%/yr., and is currently at nearly 20 million metric tons/yr.[1] Commercially, EO is produced by the $\mathbf{O_2}$-based oxidation of ethylene over a supported silver catalyst in fixed-bed reactors. The ethylene conversion per pass is maintained at 4–8% to minimize the burning of ethylene and EO, and to avoid the formation of flammable vapors. Furthermore, inert gases such as CH_4, Ar, N_2 and CO_2 are deployed to reduce the flammability envelopes associated with ethylene/EO/Air mixtures.[2–4] Despite advances in the heterogeneous silver-based catalyst formulations, the selectivity toward EO is reported to be around 85% with up to 15% of the byproducts being CO_2.[5] The CO_2 emitted as byproduct in the conventional EO process is approximately 3.4 million metric tons/yr., making it the second largest emitter of CO_2 as byproduct among all chemical processes after ammonia synthesis. More importantly, the selectivity loss as CO_2 translates into an ethylene feedstock loss of approximately $1.1 billion/yr. assuming an ethylene feedstock price of 32 ¢/lb. Increases in ethylene price, predicted to double within the next decade, will only exacerbate this loss. The rising cost of ethylene and the expansion of EO demand prompted researchers at the Center for Environmentally Beneficial Catalysis (CEBC) to develop an alternative process that conserves the ethylene feedstock and is more energy efficient.[4,6,7]

In the proposed process concept (hence, referred as the CEBC-EO process) (Figure 1), EO is produced by the selective oxidation of ethylene with hydrogen peroxide (H_2O_2) using a homogeneous catalyst, methyl trioxorhenium, MTO. Compressed ethylene gas (roughly 40–50 bar) is mixed with a liquid-phase reaction mixture containing water, methanol, hydrogen peroxide (oxidant), MTO and a promoter, pyridine N-oxide ($PyNO_x$) in the 20–40°C range.[4,6] The MTO transfers an oxygen atom from H_2O_2 to ethylene, selectively forming EO. The elimination of burning conserves feedstock and reduces the carbon footprint. Also, H_2O_2 is stable at these operating conditions such that the vapor phase is devoid of oxygen, confirmed by gas chromatographic analysis. Also, the EO product, which is flammable in the gas phase, remains dissolved in the liquid phase at the operating pressure. The virtual elimination of O_2 and EO in the vapor phase makes the process *inherently safe*.

It must be noted that in the CEBC-EO process, the reaction occurs in a gas-expanded liquid phase wherein the substrate (ethylene itself) is used as the expansion gas to increase its availability in the liquid phase. The concept is similar to how propylene (the reactive substrate) was exploited as the expansion medium in our earlier work.[6] This work is, thus, complementary to the H_2O_2-based olefin epoxidations in supercritical CO_2 or CO_2-expanded liquid phases that have been previously reported.[8–10]

Additional Supporting Information can be found in the online version of this article.

Correspondence concerning this article should be addressed to B. Subramaniam at bsubramaniam@ku.edu.

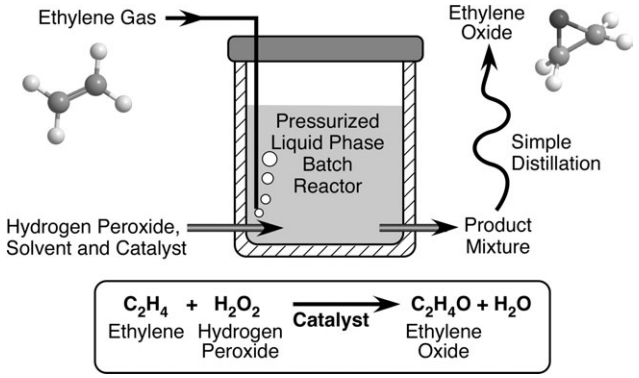

Figure 1. Schematic of the CEBC expanded-phase EO process

A number of similarities exist between the CEBC-EO process and the Dow/BASF hydrogen peroxide/propylene oxide (HPPO) process:[11] (1) methanol is employed as the cosolvent, (2) H_2O_2 is the oxidant, and (3) the operating pressures (tens of bars) and temperatures (25–40°C) in both the processes are similar.[4,6,7] Under reaction conditions, ethylene (P_c = 50.76 bars, T_c = 9.5°C) and propylene (P_c = 46.1 bars; T_c = 91°C) are both relatively close to their critical points. Hence, their solubilities in the methanol-containing liquid phase are substantial,[12] actually resulting in the formation of gas-expanded liquids (GXLs). The economic viability of the HPPO process is in major part due to the relatively high-profit margins enjoyed by PO and the relatively inexpensive catalyst (Ti-based), factors that effectively offset the cost of using H_2O_2 as oxidant. In contrast, the rhenium-based catalyst is expensive making EO profit margins lower and the economic viability of the CEBC-EO process more challenging. However, recent developments in the cost-effectiveness and greener syntheses of both H_2O_2 and the MTO catalyst provide justification for continued investigations aimed at improving the commercial viability of this technology.

Conventionally, H_2O_2 has been produced by the standard anthraquinone process, a highly energy intensive technology.[11,13,14] In recent years, significant advances in the development of alternative H_2O_2 processes have been reported to lower the cost of H_2O_2 production. Solvay commercialized the high-productivity amylanthraquinone technology,[15] and the direct H_2O_2 process has been demonstrated at the pilot-plant scale by a joint venture between Evonik Degussa and Udhe, Inc.[16] The MTO catalyst is a highly versatile epoxidation catalyst and is known to catalyze a broad spectrum of oxygen transfer reactions.[17–19] The mechanism of oxygen transfer in the MTO/H_2O_2 system has been extensively studied.[20,21] In the presence of excess H_2O_2, the MTO catalyst remains in the highly active diperoxo form. Yin and Busch recently reported that the formation of the mono-peroxo complex by the MTO catalyst as the primary pathway for the destruction of MTO catalyst.[22] Consequently, in the presence of excess H_2O_2, the preferred active species (diperoxo complex) has the potential to be indefinitely stable. Recently, Hermann et al. reported a greener, cost-effective process for the synthesis of MTO that has the potential to reduce the cost of the catalyst.[23]

For rational development and economic assessment of the CEBC-EO process, fundamental engineering data are essential. This article is focused on understanding the thermodynamics, mass-transfer rates, and intrinsic epoxidation kinetics associated with the dissolving of ethylene and its subsequent conversion in its self-expanded liquid phase. Herein, the volumetric expansion of the liquid reaction phase by pressurized ethylene is quantitatively established. Based on the measured ethylene dissolution rates into the liquid phase at constant pressure and temperature but different agitation speeds, gas-liquid mass-transfer coefficients were estimated from a mathematical model of the stirred semibatch system. The ethylene epoxidation reactions were reinvestigated in the absence of mass transfer limitations to quantify the enhancement of EO yield, and also obtain intrinsic kinetic parameters from temporal conversion and selectivity profiles.

Experimental

Materials

Ethylene was purchased from Matheson Tri-Gas Co., (ultrahigh-purity grade). The MTO (71.0–76.0 wt % Re), oxidant (50 wt % H_2O_2 in H_2O), methanol (HPLC grade, $\geq$ 99.99%), ferroin indicator solution, acetonitrile (HPLC grade $\geq$ 99.9%) and pyridine N-oxide (95%) were purchased from Sigma-Aldrich and used without further purification. Ceric sulfate (0.1 N) was purchased from Fisher Scientific. Trace metal grade sulfuric acid (99.9 wt %) purchased from Fisher Scientific was diluted to 5% (v/v) H_2SO_4 solution. Hydranal composite 5, one component reagent for volumetric titration of H_2O is purchased from Riedel-de-Haen. Ethylene oxide and anhydrous ethylene glycol standards were purchased from Supelco Analytical and Sigma-Aldrich, respectively.

Apparatus and procedure

Volumetric Expansion Studies. The high solubility of compressed ethylene in methanol leads to the formation of ethylene-expanded liquids. Volumetric expansion studies were conducted in a 50 cm^3 high-pressure Jurgeson cell designed to withstand a pressure of 400 bar at 100°C.[24] Either methanol (solvent) or methanol + 50% H_2O_2/H_2O mixture is loaded into the view cell, immersed in a constant temperature bath. Ethylene is charged into the cell from an external reservoir through a two-stage pressure regulator, maintaining the Jurgeson cell at a constant pressure. The attainment of equilibrium is facilitated by mixing the gas and liquid phases with the aid of a piston that can be moved vertically within the cell across the two phases and a magnetic stirrer bar in the liquid phase. The volume of the ethylene-expanded liquid phase at equilibrium is measured visually on a calibrated linear scale attached to the view cell.[25]

Mass-Transfer Investigations. These studies were conducted in a 50 mL Parr reactor setup (Figure 2). The

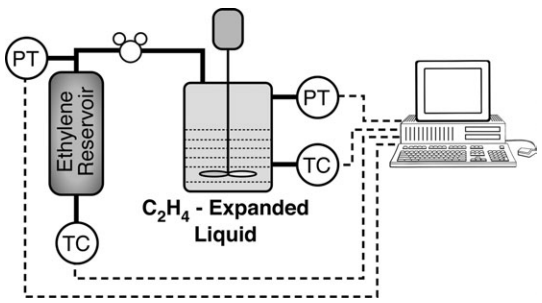

Figure 2. Schematic of stirred semibatch mixer unit to measure the ethylene transport rates into the liquid phase.

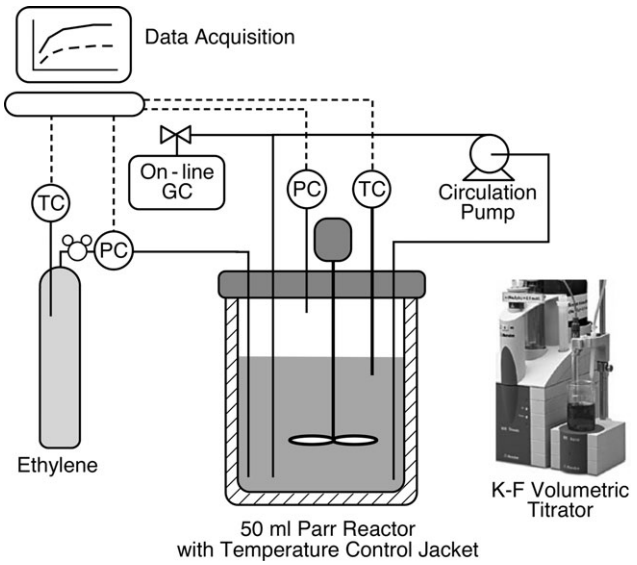

Figure 3. Schematic of the experimental setup for ethylene epoxidation studies in gas-expanded liquid phase.

pressure and temperature in the reactor are monitored using LabView 7.0® data acquisition software. Ethylene is charged into the reactor from an external reservoir, maintained at ambient temperature, through a two-stage pressure regulator that maintains the reactor pressure constant at 50 bars. The decrease in the external reservoir pressure, a direct measure of ethylene uptake in the Parr reactor, is also logged by the LabView 7.0® software.

Kinetic Studies in Gas-Expanded Liquid Phase. The schematic of the reactor setup for the epoxidation studies is shown in Figure 3. Ethylene epoxidation reactions were conducted in semicontinuous mode in a 50 mL Parr reactor equipped with a magnetically driven stirrer, a pressure transducer and a thermocouple. The reactor temperature is controlled between 20–40°C by a circulating water bath. The impeller speed is maintained at 1,200 rpm to ensure the absence of mass-transfer resistances. A micropump (model # 415A) circulates the reaction mixture at a flow rate of approximately 30 mL/min to facilitate the sampling of the ethylene-expanded liquid phase for analysis. A solution containing 50% H_2O_2/H_2O (0.268 mol), pyridine N-oxide (1.82 mmol) and MTO (0.18–0.54 mmol) dissolved in CH_3OH (30 mL), and internal standard CH_3CN (1 mL), was charged into the reactor and ethylene was injected from an external reservoir pressurizing the reactor up to 50 bars.[4] The reactor pressure was maintained constant by continuously replenishing the consumed ethylene from the external ethylene reservoir. Isothermal, constant pressure semibatch reactions lasting up to 5 h were carried out at several temperatures in the 20–40°C range. The gas-expanded liquid phase was sampled at regular time intervals. The H_2O_2 and H_2O contents of the liquid phase were quantified by Ceric Sulfate and Karl Fischer titrations, respectively.[26–29] Details of the GC analysis, ceric sulfate titration and Karl Fischer titration are provided as part of the Supplementary Materials (see online for additional Supplementary Material).

In the presence of a molar excess of H_2O_2 (with respect to the catalyst), the MTO catalyst is present as the highly active di(peroxo) rhenium complex that selectively transfers an oxygen atom to ethylene to form EO.[18,21] The reaction order with respect to catalyst concentration was established by varying the catalyst amount (from 0.180–0.542 mmol). The intrinsic kinetic parameters (k', E) for ethylene epoxidation were estimated from the temporal concentration profiles (of EO, H_2O_2 and H_2O) at different temperatures by regression with a pseudo-first-order kinetic model based on conversion of the limiting reactant (H_2O_2) to EO in the presence of excess ethylene (maintained at a constant concentration) and constant catalyst concentration.

Results and Discussion

Volumetric expansion studies

Reliable estimation of interphase gas-liquid mass-transfer coefficients is vital for rational process development. Unlike conventional liquid phases, gas-expanded liquid phases are compressible depending on the extent of gas dissolution into the liquid phase. The volumetric expansion data are essential to accurately account for the dilution caused by the enhanced ethylene dissolution in the liquid phase, and, therefore, to reliably interpret conversion and selectivity data used to obtain kinetic parameters.

The volumetric expansion ratio is defined as the equilibrium volume of the expanded liquid phase at temperature T and pressure P, relative to the volume (V_o) of the unexpanded phase at 1 atm and the same T[25]

$$\frac{V(T,P)}{V_o(T,P_o)} \tag{1}$$

In the 20–40°C temperature range, the solubility of ethylene in the liquid phase is substantial at pressures in the vicinity of the critical pressure of ethylene ($P_c = 50.76$ bar). As shown in Figures 4a and 4b, the volume of the initial liquid phase, containing either methanol alone or a representative reaction mixture containing 0.748 mol methanol + 0.134 mol H_2O_2 + 0.253 mol H_2O, increases with increasing ethylene pressure. For the ethylene+methanol system, the expansion shows the characteristic exponential dependence as the critical pressure of ethylene is approached. At a fixed pressure, the volumetric expansion of the liquid phase decreases with increasing temperature due to the lower gas solubility at higher temperatures. The maximum volumetric expansion ratios for the ethylene+methanol system at approximately 50 bars and at 20, 30 and 40°C are 1.89, 1.62 and 1.50, respectively, signifying substantial increases in the liquid-phase volume on ethylene addition. The corresponding mole fractions (x_E) of ethylene in the liquid phase are 0.309, 0.216 and 0.163, respectively. These values are consistent with the reported VLE behavior of this binary system and previously predicted values.[12] In comparison, the ethylene mole fraction in methanol phase at 20°C and 1 bar is 0.052.

The expansion ratios in the ternary mixture (containing methanol, H_2O_2 and H_2O) at similar conditions are comparatively lower, albeit significant, being 1.17, 1.15 and 1.13, respectively. Furthermore, the volumetric expansion profile is linear in the pressure range reflecting the fact that ethylene is less soluble in the presence of water. The corresponding mole fractions of ethylene are 0.0216, 0.017 and 0.0141. In comparison, the ethylene mole fraction in water at 20°C and 50 bars is $1.96(10^{-3})$.

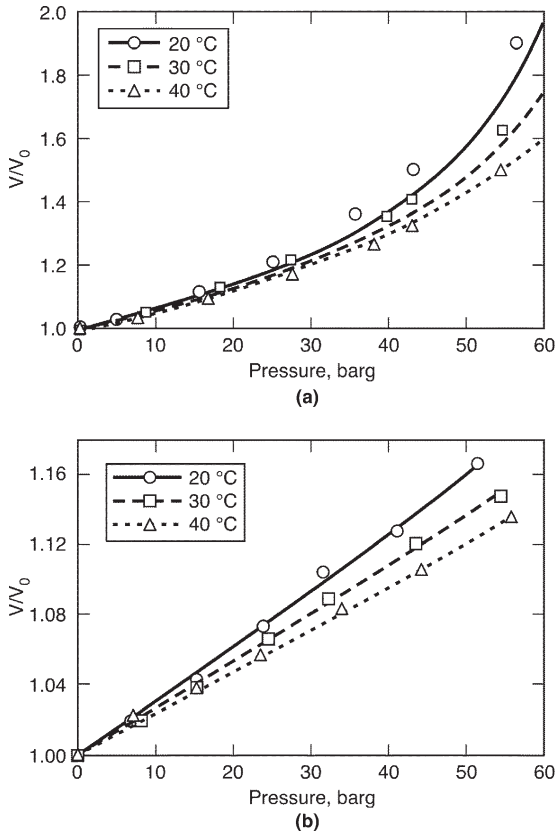

Figure 4. Isothermal volumetric expansion of liquid phases upon pressurization by ethylene.

(a) Ethanol + methanol binary system; (b) (ethylene + methanol + 50 wt % H_2O_2/H_2O) ternary system. Initial composition of liquid phase = 0.748 mol methanol + 0.134 mol H_2O_2 + 0.253 mol H_2O. Initial volume of liquid phase = 15 mL. The size of the plotted data points represents the experimental uncertainty.

It must be noted that the minor components (MTO catalyst and $PyNO_x$ promoter) are soluble in the reaction mixture, but constitute less than 0.005 wt % of the initial reaction mixture. To avoid reaction, MTO and PyNO were not included in the aforementioned volumetric expansion studies. Furthermore, EO was also not included in the expansion studies since the EO formed during the reaction constitutes only 4.5 wt % of the reaction mixture even at the highest conversion (at the catalyst loading of 0.54 mmol), remaining mostly in the liquid phase at typical reaction conditions.[30]

Mass-transfer studies involving gas-expanded phases

The volumetric mass-transfer coefficient is experimentally determined by conducting ethylene uptake experiments as explained in the Experimental section. The transient pressure profiles from the reservoir provide a direct measure of the rate at which ethylene dissolves into the liquid phase. At 25°C and 50 bars, the rate of ethylene dissolution into the liquid phase increases with stirring speed indicating the presence of gas-liquid mass-transfer limitations (Figure 5). The ethylene uptake by the liquid phase reaches equilibrium asymptotically at sufficiently high stirring rates (> 1,000 rpm). Beyond 1,200 rpm, there is no observed change in the slope of the pressure profiles indicating that interphase mass-transfer limitations are no longer significant. Furthermore, at stirrer speeds exceeding 1,200 rpm, approximately 99% of the equilibrium solubility is attained within 100 s. At 50 bars and 25°C, the measured equilibrium mole fraction of ethylene in the liquid phase is 0.21, which closely matches the published value.[12] Using this technique, the equilibrium mole fractions of ethylene in the ternary mixture (0.748 mol methanol + 0.1344 mol H_2O_2 + 0.253 mol H_2O) at 50 bars was found to be 0.108 and 0.0405 at 25 and 35°C, respectively. In comparison, the equilibrium mole fraction of ethylene in water at 35°C, and 50 bar ethylene pressure is 1.96 (10^{-3}).[31] This remarkable solubility enhancement by more than an order of magnitude in methanol-based reaction mixtures under moderate compression renders ethylene as the stoichiometrically excess reactant in the gas-expanded liquid phase. For reference, the corresponding mole fractions of H_2O_2 in the ethylene-expanded liquid phase at 50 bars are 0.061 at 25°C and 0.0615 at 40°C.

A mathematical model was developed to estimate the mass-transfer coefficient (k_la) of the system. The model assumes instantaneous equilibrium at *the gas-liquid interface* for the solubility of ethylene in either methanol or the ternary mixture (73.6 wt % methanol +13.2 wt % H_2O_2 + 13.2 wt % H_2O). At constant pressure, the depletion of ethylene in the external reservoir equals the rate at which ethylene dissolves into the gas phase. A differential mass balance for ethylene in the isothermal, constant pressure semibatch mixer yields

$$-\left(\frac{V_R}{RT}\right)\left(\frac{dP_g}{dt}\right) = k_l a\left(C_E^* - C_{EL}\right)V_L \tag{2}$$

Initial condition $t = 0$, $P = P_{g,I}$.

Substituting for C_E^* and C_{EL} in terms of the gas-phase ethylene partial pressures

$$-\left(\frac{dP_g}{dt}\right) = k_l a\left[\frac{\phi PRTV_L}{P_s\gamma_i V_m V_R} - P_{g,I} + P_g\right] \tag{3}$$

Solution of the equation (details provided in Appendix B in online Supplementary Materials) results in the following linearized equation.[32] Details of the methodology to estimate the gas-phase fugacity coefficient and liquid-phase activity

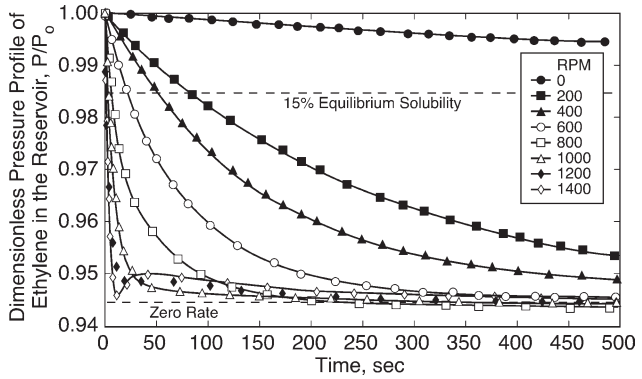

Figure 5. Effect of stirring speed on the uptake of compressed ethylene by the liquid phase.

***P* = 50 bar; *T* = 25°C; Initial composition of the liquid phase: 0.748 mol methanol + 0.1344 mol H_2O_2 + 0.253 mol H_2O.**

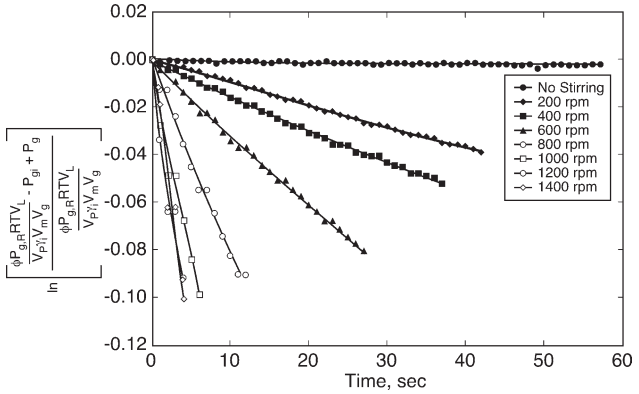

Figure 6. Regressed ethylene uptake profiles at various stirring speeds using first-order model.

Slopes provide the mass-transfer coefficients.

coefficient are shown in Appendix D of the Supplementary Materials[33,34]

$$\ln\left[\frac{\frac{\phi PRTV_L}{P_s\gamma_i V_m V_R} - P_{g,I} + P_g}{\frac{\phi PRTV_L}{P_s\gamma_i V_m V_R}}\right] = k_l a t \tag{4}$$

Reliable estimations of $k_l a$ were obtained by regressing transient ethylene pressure profiles corresponding to low-uptake values (up to 15% of equilibrium values), where the difference in mass-transfer rates at various stirring speeds is easily discerned. Furthermore, at these levels of ethylene uptake, the volumetric expansion is low (< 2%), and, hence, the assumption of constant liquid-phase volume is valid. By plotting the observed P_g vs. t values according to Eq. 4, linear plots are obtained (Figure 6), confirming the first-order nature of the mass-transfer process. As shown in Figure 7, the $k_l a$ values (slopes of the plot in Figure 6) increase with stirring and reach an asymptotic value beyond 1,200 rpm.

The values of the volumetric mass-transfer coefficients ($k_l a$) for the ethylene + methanol (binary) and ethylene + 0.748 mol methanol + 0.1344 mol H_2O_2 + 0.253 mol H_2O (quaternary) systems are summarized in Table 1. At 1,200 rpm, the $k_l a$ values for these systems are 0.0135 s^{-1} and 0.0082 s^{-1}, respectively. It must be noted that when increasing the stirring speed from 400 rpm to 1,200 rpm, the volumetric mass-transfer coefficient increases by threefold for the binary system, and by a factor of 1.6 for the quaternary system. Consequently, enhanced EO yields were observed in the absence of mass-transfer limitations. As seen in Figure 8, the temporal EO yields at 40°C and 50 bars are enhanced several-fold at 1,200 rpm compared to operation at 400 rpm. At the end of 5 h, the EO yield obtained at 1,200 rpm (0.049 mol) is more than an order of magnitude greater than that obtained at 400 rpm.

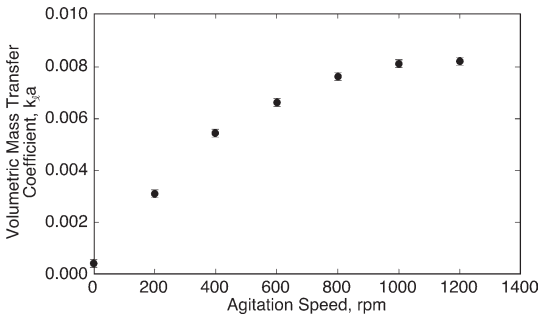

Figure 7. Variation of volumetric mass-transfer coefficient with stirring speed.

P = 50 bars; T = 25°C; Initial composition of the liquid phase: 0.748 mol methanol + 0.134 mol H_2O_2 + 0.253 mol H_2O.

Table 1. Volumetric Mass-Transfer Coefficients for Ethylene+Methanol Binary Mixture and Ethylene + 0.748 mol Methanol + 0.134 mol H_2O_2 + 0.253 mol H_2O Quaternary Mixture

	Volumetric Mass Transfer Coefficient ($\times$1000, s^{-1})	
Agitation speed (rpm)	Ethylene+ Methanol,	Ethylene+Methanol $+H_2O_2/H_2O$
0	0.49	0.32
200	1.81	5.12
400	4.92	5.42
600	7.31	6.32
800	10.21	7.61
1000	12.12	8.12
1200	13.21	8.21
1400	13.22	8.22

Kinetic analysis

The temporal conversion and selectivity measurements for estimating kinetic parameters were obtained from fixed-time semibatch studies, ensuring that interphase mass-transfer limitations are eliminated. The effect of catalyst concentration on EO yield was first investigated by varying the catalyst concentration in the liquid phase. As shown in Table 2, the moles of EO formed, H_2O_2 consumed and H_2O formed are within 5–10% in most cases, consistent with the reaction stoichiometry. Furthermore, the EO yield increases nearly linearly with catalyst loading (0.180–0.54 mmol) suggesting first-order dependence with respect to catalyst concentration. In the presence of excess H_2O_2 (molar oxidant/catalyst ratio >10), the MTO catalyst is present as the highly active diperoxo complex.[21] In our experiments, the molar oxidant (H_2O_2)/catalyst (MTO) ratio ranges from 34–102, which favors the formation of the more active and stable diperoxo complex. The enhanced epoxidation rates at higher catalyst

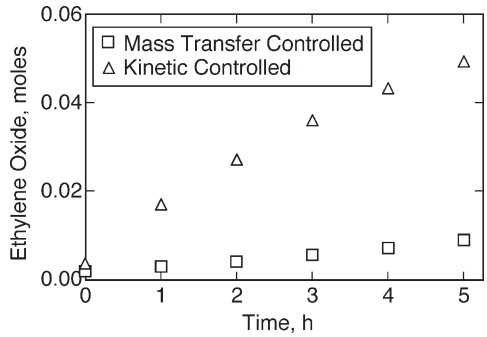

Figure 8. EO yield in the presence and absence of mass-transfer limitations.

Ethylene P = 50 bars; T = 40°C; MTO amount = 0.361 mmol; methanol = 0.748 mol; H_2O_2 = 0.116 mol; H_2O = 0.220 mol; acetonitrile = 0.0191 mol; pyridine *N*-oxide = 2.19 mmol; batch time = 5 h; agitation speed (Ä: 1,200 rpm, ≤ □: 400 rpm).

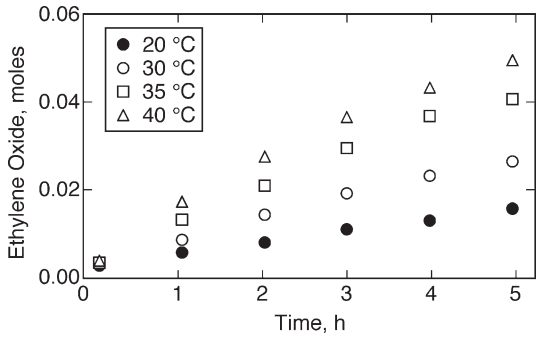

Figure 9. EO yields in the absence of mass-transfer limitations.

***P* = 50 bars; *T* = 40°C; agitation speed = 1,200 rpm; MTO amount = 0.361 mmol; methanol = 0.748 mol; H_2O_2 = 0.116 mol; H_2O = 0.220 mol; acetonitrile = 0.0191 mol; pyridine *N*-oxide = 2.19 mmol.**

loadings are, therefore, attributed to the greater concentration of the active diperoxo species. It must also be noted that in the wide range of conversions studied at the various temperatures, GC/FID analysis did not show any detectable peak other than EO. It is, therefore, concluded that the concentrations of the oxygenated products other than EO are on the order of a few ppm at most. The absence of the ring opening reaction to produce ethylene glycol is attributed to the presence of pyridine N-oxide. This weak base prevents the acid-catalyzed ring opening reaction.[6]

Kinetic measurements were performed with a fixed catalyst loading of 0.36 mmol at 50 bars and in the 20–40°C temperature range. At these conditions, the ethylene concentration in the liquid phase is typically in excess. Continuous ethylene replenishment in the reactor to maintain constant pressure ensures that the ethylene excess is maintained throughout the reaction. At these conditions, the end-of-run ($\sim$ 5 h) EO yield increases from 0.015 mol to 0.049 mol as the reaction temperature is increased from 20 to 40°C (Figure 9). The EO yield and selectivity at 40°C and 50 bars are 50% (based on H_2O_2 converted) and >98%, respectively.

For the kinetic analysis, the rate of EO formation is assumed to be first-order with respect to the concentrations of ethylene (C_{EL}), hydrogen peroxide ($C_{H_2O_2}$), and the catalyst (C_{cat}). Given that the catalyst and ethylene concentrations in the liquid phase are maintained constant, the EO yield vs. time data were regressed with a simple, constant-density, pseudo first-order model for EO formation as follows:

$$\left(\frac{dC_{EO}}{dt}\right) = k' C_{H_2O_2,t} \tag{5}$$

where $k' = kC_{EL}\, C_{\text{cat}}$.

Table 2. Effect of Catalyst Loading on H_2O_2 Consumption and Product Yields

Catalyst, mmol	EO yield, mol	H_2O_2 consumed, mol	H_2O produced, mol
0.180	0.0248	0.0278	0.0234
0.361	0.0493	0.0478	0.0507
0.542	0.0697	0.0710	0.0698

P = 50 bars; *T* = 40°C; agitation speed = 1,200 rpm; methanol = 0.748 mol; H_2O_2 = 0.116 mol; H_2O = 0.220 mol; acetonitrile = 0.0191 mol; pyridine *N*-oxide = 2.19 mmol; batch time = 5 h.

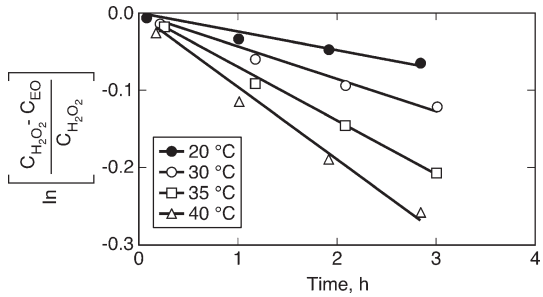

Figure 10. Regression of temporal EO yields based on a pseudo first-order kinetic model.

***P* = 50 bars; *T* = 40°C; agitation speed = 1,200 rpm; MTO amount = 0.361 mmol; methanol = 0.748 mol; H_2O_2 = 0.116 mol; H_2O = 0.220 mol; acetonitrile = 0.0191 mol; pyridine *N*-oxide = 2.19 mmol; batch time = 5 h.**

Recognizing that the moles of EO formed should equal the moles of H_2O_2 converted

$$C_{H_2O_2,t} = C_{H_2O_2,0} - C_{EO,t} \tag{6}$$

Substituting Eq. 6 into Eq. 5 yields

$$\left(\frac{dC_{EO}}{dt}\right) = k'\left(C_{H_2O_2,0} - C_{EO,t}\right) \tag{7}$$

Applying the initial condition: $t = 0$, $C_{E,0} = 0$, the solution to Eq. 7 is given by:

$$-\ln\left[\frac{C_{H_2O_2,0} - C_{EO,t}}{C_{H_2O_2,0}}\right] = k't \tag{8}$$

The pseudo first-order rate constant for the ethylene epoxidation system is estimated from temporal conversion and selectivity data, where the H_2O_2 conversion (and hence EO yield) is less than 15%. As inferred from Figure 10, the linearity of the data at each temperature, plotted according to Eq. 8, validates the assumption of pseudo-first-order kinetics. The pseudo first-order rate constants (k'), estimated from the slopes, are tabulated in Table 3. Arrhenius plot of these rate constants yields moderate activation energy of 57 $\pm$ 2 kJ/mol (Figure 11) with a pre-exponential factor of 3.8 (10^7) s^{-1}.

At 50 bars and 40°C, the volumetric mass-transfer coefficient ($k_l a$) and the epoxidation rate constant (k') under the operating condition are 0.0082 s^{-1} (Table 2), and 2.64(10^{-5}) s^{-1} (Table 3), respectively. The ratio of the observed reaction rate (R_{EO}, estimated from the slope of the temporal EO formation profile at early time) and the estimated reaction rate under mass-transfer limitations (i.e., the product of the volumetric mass-transfer coefficient and maximum concentration of H_2O_2 in the liquid phase) is 3.21(10^{-3}). This value

Table 3. Rate Constants for the Liquid Phase CEBC-EO Process (*P* = 50 bars)

Temperature, °C	Rate constant *k*', s^{-1}
20	6.2 (10^{-6})
30	1.18 (10^{-5})
35	1.85 (10^{-5})
40	2.64 (10^{-5})

is significantly less than the empirical criterion for the elimination of mass-transfer limitations shown in Eq. 9.[35]

$$\alpha = \frac{R_{EO}}{k_l a C_{H_2O_2}} < 0.1 \tag{9}$$

Comparison with conventional process

Table 4 compares the CEBC-EO process to the conventional vapor-phase ethylene epoxidation process. The EO yield and selectivity at 40°C and 50 bars are 50% (based on H_2O_2 converted) and >98%, respectively. The process conditions (50 bars, 20–40°C) in the proposed CEBC-EO process are moderate and the ethylene productivity 1.61–4.97 (g EO/h/g metal) is comparable to that observed in the conventional process 2.2–4.1 (g EO/h/g metal).[5] Furthermore, the CEBC process is highly selective toward the desired product EO, and no CO_2 is detected as byproduct in either the gas or liquid phases. The efficient utilization of ethylene feedstock has the potential to make the CEBC-EO process economically favorable. However, H_2O_2 is more expensive than O_2 as oxidant and this cost must be offset by not only the savings from better utilization of feedstock, but also reduced operating expenses. The ethylene separation and recompression costs in the conventional process are rather high due to the rather low (4–8%) per pass conversion, necessitated by the propensity of ethylene and EO to form highly flammable vapors in the presence of air. In contrast, the vapor phase in the CEBC-EO process contains no O_2, and the EO remains substantially dissolved in the liquid phase at the operating conditions. The absence of flammable vapor in the gas phase makes the process inherently safe. This also means that the ethylene conversion per pass is not constrained in the CEBC-EO process, which should significantly lower the ethylene purification and recycle costs. These avenues for cost savings are being investigated via comparative economic analyses of the CEBC-EO process and the conventional process. Cradle-to-gate life cycle assessments are also underway to assess if the savings in CO_2 emissions (as a byproduct), achieved in the CEBC-EO process, are offset by CO_2 emissions resulting from either increased power consumption or from the use of other reagents that produce CO_2 as byproduct (e.g., H_2O_2 production).

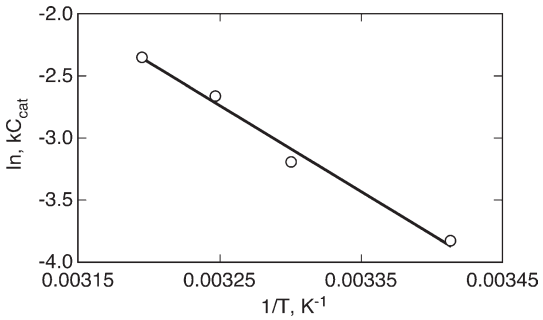

Figure 11. Arrhenius plot for EO formation via the CEBC-EO process.

***P* = 50 bars; *T* = 40°C; agitation speed = 1,200 rpm; MTO amount = 0.361 mmol; methanol = 0.748 mol; H_2O_2 = 0.116 mol; H_2O = 0.220 mol; acetonitrile = 0.0191 mol; pyridine *N*-oxide = 2.19 mmol; batch time = 5 h.**

Table 4. Comparison of Key Parameters and Performance Metrics in the Conventional and CEBC-EO Processes

	Conventional Process*	CEBC Process
Pressure, bars	10-20	50
Temperature, °C	200-300	20-40
Conversion	10% per pass	50% per batch
EO Selectivity	80-90%	99+%
CO_2 byproduct	10-20%	No CO_2 detected
Productivity, g EO/h/g of active metal	2.2-4.1	1.61-4.97

Reference 5.

Conclusion

A liquid-phase homogeneous catalytic process for selective ethylene epoxidation that operates at mild process conditions uses benign reagents and completely eliminates ethylene and/or burning to CO_2 has been fully characterized with respect to the underlying thermodynamics, mass transfer rates and intrinsic kinetics. The activation energy for ethylene epoxidation by methyltrioxorhenium catalyst using H_2O_2 as oxidant and PyNO as promoter is moderate (+ 57 ± 2 kJ/mol). These fundamental investigations have helped optimize operating conditions (P, T, stirring speed) to enhance the ethylene solubility and its rate of dissolution in the liquid phase, and, thereby, to maximize the EO productivity. The EO productivity in the CEBC-EO process is comparable to that in the conventional EO process.

The complete utilization of ethylene to produce EO and the inherently safe nature of the CEBC-EO process provide a stimulus for identifying the major economic drivers and establishing performance benchmarks (e.g., catalyst life and durability, H_2O_2 cost, reduction in CO_2 emissions, etc.) for economic viability. Indeed, successful commercialization of such processes is needed to promote sustainability in the chemical industry.

Acknowledgments

This work was partly supported with funds from the NSF Engineering Research Centers Grant EEC-0310689.

Notation

C^*_E = concentration of ethylene at the gas-liquid interface, mol L^{-1}
C_{EL} = concentration of ethylene in the liquid phase at any time, mol L^{-1}
$C_{EO,t}$ = concentration of ethylene oxide at time t, mol L^{-1}
$C_{H_2O_{2,0}}$ = initial (t = 0) concentration of hydrogen peroxide in the liquid phase, mol L^{-1}
$C_{H_2O_{2,t}}$ = concentration of hydrogen peroxide at time t, mol L^{-1}
E = activation energy, kJ mol^{-1}
$k_l a$ = gas-liquid mass-transfer coefficient, s^{-1}
k = intrinsic rate constant for epoxidation reaction, L mol^{-1} s^{-1}
k' = kC_E pseudo first-order rate constant, s^{-1}
P = reactor pressure held constant at a predetermined value, bar
P_g = pressure in the external ethylene reservoir at time t, bar
$P_{g,I}$ = initial ethylene pressure in the external reservoir, bar
P_s = saturation vapor pressure of ethylene at reactor pressure and temperature, bar
R = universal gas constant, 0.082057 L bar^{-1} mol^{-1} K^{-1} or $1.985(10^{-3})$ Kcal mol^{-1} K^{-1} (or) $0.08314(10^{-3})$ KJ mol^{-1} K^{-1}
r_{EO} = rate of ethylene oxide formation, mol L^{-1} s^{-1}
T = reactor temperature, °C or K
t = elapsed time from the start of an experiment, s^{-1}
V_L = liquid-phase volume at time t, L
V_m = molar volume of the liquid phase, mol L^{-1}
V_R = volume of the external ethylene reservoir, L

V_0 = initial ($t = 0$) volume of the liquid phase in the reactor, L
x_E = mole fraction of ethylene in the liquid phase
y_E = mole fraction of ethylene in the gas phase

Greek letters

ϕ = gas-phase fugacity coefficient of ethylene (see online in Supplementary Materials)
γ = liquid-phase activity coefficient of ethylene (see online in Supplementary Materials)

Literature cited

1. ICIS. www.icispricing.com. Accessed June, 2010.
2. Zabetakis MG. *Flammability Characteristics of combustible gases and vapors*. US Dept of the Interior, US Bureau of Mines; 1965.
3. Rebsdat S, Mayer D. *Ethylene Oxide*. In: Hawkins S, Russey WE, Pilkart-Muller M, eds. *Ullmann's Encyclopedia of Industrial Chemistry*. 6th ed. New York: Wiley-VCH; 2005;13:23.
4. Lee HJ, Ghanta M, Busch DH, Subramaniam B. Towards a CO_2-free ethylene oxide process: Homogeneous ethylene oxide in gas-expanded liquids. *Chem Eng Sci*. 2010;65:128–134.
5. Buffum JE, Gerdes WH, Kowaleski RM. Ethylene Oxide Catalyst. US Patent 5,145,824. 1992.
6. Lee HJ, Shi TP, Busch DH, Subramaniam B. A greener, pressure intensified propylene epoxidation process with facile product separation. *Chem Eng Sci*. 2007;62:7282–7289.
7. Subramaniam B, Busch DH, Lee HJ, Ghanta M, Shi T-P. Process for selective oxidation of olefins to epoxides. US CIP Patent application 11/586,061. August 9, 2011.
8. Hancu D, Green H, Beckman EJ. H_2O_2 in CO_2/H_2O biphasic systems: Green synthesis and epoxidation reactions. *Ind Eng Chem Res*. 2002;41:4466–4474.
9. Hancu D, Green J, Beckman EJ. H_2O_2 in CO_2: Sustainable production and green reactions. *Acc Chem Res*. 2002;35:757–764.
10. Nolen SA, Lu J, Brown JS, Pollet P, Eason BC, Griffith KN, Glaser R, Bush D, Lamb DR, Liotta CL, Eckert CA, Thiele GF, Bartels KA. Olefin epoxidations using supercritical carbon dioxide and hydrogen peroxide without added metallic catalysts or peroxy acids. *Ind Eng Chem Res*. 2002;41:316–323.
11. Pujado PR, Hammerman JI. Integrated process for the production of propylene oxide. US Patent 5,599,956. 1997.
12. Ohgaki K, Nishii H, Saito T, Katayama T. High-Pressure phase equilibria for the methanol-ethylene System at 25 C and 40 C. *J Chem Eng Jpn*. 1983;16:263–267.
13. Durst RA, Bates RG. *Hydrogen Peroxide* In: Eul W, Moeller A, Steiner N, eds. *Kirk-Othmer Encyclopedia of Chemical Technology*. 5th ed. Hoboken, NJ: John Wiley, Inc; 2007;14:32.
14. Goor G, Glenneberg J, Jacobi S. *Hydrogen Peroxide*. In: *Ullmann's Encyclopedia Of Industrial Chemistry*. 6th ed. Wiley VCH: 2007;18:35.
15. ChemSystems. http://www.chemsystems.com/about/cs/news/items/PERP%200708_3_Hydrogen%20Peroxide.cfm. Accessed July 27, 2011.
16. Zhou B, Rueter M, Parasher S. Supported catalysts having a controlled coordination structure and methods for preparing such catalysts. US Patent 7,011,807 B2. 2006.
17. Sharpless BK, Yudin AK. Epoxidation of olefins. US Patent 6,271,400. 2001.
18. Espenson JH, AbuOmar MM. Reactions catalyzed by methylrhenium trioxide. *Elect Trans React*. 1997;253:99–134.
19. Romao CC, Kuhn FE, Herrmann WA. Rhenium(VII) oxo and imido complexes: Synthesis, structures, and applications. *Chem Rev*. 1997;97:3197–3246.
20. Owens GS, Aries J, Abu-Omar MM. Rhenium oxo complexes in catalytic oxidations. *Catal Today*. 2000;55:317–363.
21. AbuOmar MM, Hansen PJ, Espenson JH. Deactivation of methylrhenium trioxide-peroxide catalysts by diverse and competing pathways. *J Am Chem Soc*. 1996;118:4966–4974.
22. Yin G, Busch DH. Mechanistic details to facilitate applications of an exceptional catalyst, methyltrioxorhenium: Encouraging results from oxygen-18 isotopic probes. *Catal Lett*. 2009;130:52–55.
23. Tosh E, Mitterpleininger JKM, Rost AMJ, Veljanovski D, Herrmann WA, Kuhn FE. Methyltrioxorhenium revisited: improving the synthesis for a versatile catalyst. *Green Chem*. 2007;9:1296–1298.
24. Jin H, Subramaniam B. Homogeneous catalytic hydroformylation of 1-octene in CO_2-expanded solvent media. *Chem Eng Sci*. 2004;59:4887–4893.
25. Laird B, Houndonougbo Y, Jin H, Rajagopalan B, Wong K, Kuczera K, Subramaniam B. Phase equilibria in carbon dioxide expanded solvents: Experiments and molecular simulations. *J Phys Chem B*. 2006;110:13195–13202.
26. Determination of Hydrogen Peroxide Concentration (0.1 to 5%). http://www.solvaychemicals.us/static/wma/pdf/6/6/2/5/XX-122.pdf. Accessed June 10th, 2011.
27. Hurdis EC, Romeyn H. Accuracy of determination of hydrogen peroxide by cerate oxidimetry. *Anal Chem*. 1954;26:320–325.
28. Margolis SA. Sources of systematic bias in the measurement of water by the coulometric and volumetric Karl Fischer methods. *Anal Chem*. 1997;69:4864–4871.
29. Margolis SA. Source of the difference between the measurement of water in hydrocarbons as determined by the volumetric and coulometric Karl Fischer methods. *Anal Chem*. 1999;71:1728–1732.
30. Golubev YD, Dement'eva L, VLasov GM. The Solubility of ethylene oxide in C1–4 alcohols. *Sov Chem Ind*. 1971:3.
31. Bradbury EJ, Mcnulty D, Savage RL, McSweeney EE. Solubility of ethylene in water: effect of temperature and pressure. *Ind Eng Chem*. 1952;44:211–212.
32. Chaudhari RV, Gholap RV, Emig G, Hofmann H. Gas-liquid mass-transfer in dead-end autoclave reactors. *Can J Chem Eng*. 1987;65:744–751.
33. Prausnitz JM, Lichtenthaler RN, Azevedo EGd. *Molecular Thermodynamics of Fluid-Phase Equilibria*. 3rd. ed. New York: Prentice Hall; 1999.
34. Walas SM. *Phase Equilibria in Chemical Engineering*. London, UK: Buttersworth; 1985.
35. Doraiswamy LK, Sharma MM. *Fluid–Fluid-Solid Reactions*. 1st. ed. New York: John Wiley & Sons; 1984.

Manuscript received Nov. 22, 2011, and revision received Jan. 10, 2012, and final revision received Mar. 1, 2012.